Journal of Technomaterial Physics
Journal homepage: https://talenta.usu.ac.id/JoTP

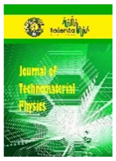

Raman Spectroscopic Analysis of Cu-Ag-In-S/CdSe Core/Shell Quantum Dots Grown on Mesoporous TiO₂ Substrates

Siti Utari Rahayu[1*] and Andy Candra[2]
[1] *Department of Physics, Faculty of Mathematics and Natural Sciences, Universitas Sumatera Utara, Jalan Bioteknologi No.1, Medan 20155, North Sumatra, Indonesia*
[2] *Department of Chemistry, Faculty of Mathematics and Natural Sciences, Universitas Sumatera Utara, Jalan Bioteknologi No.1, Medan 20155, North Sumatra, Indonesia*
*Corresponding Author: siti.utari@usu.ac.id

ARTICLE INFO

Article history:
Received 8 January 2025
Revised 30 January 2025
Accepted 5 February 2025
Available online 28 February 2025

E-ISSN: 2656-0755
P-ISSN: 2656-0747

How to cite:
S. U. Rahayu and A. Candra, " Raman Spectroscopic Analysis of Cu-Ag-In-S/CdSe Core/Shell Quantum Dots Grown on Mesoporous TiO₂ Substrates," Journal of Technomaterial Physics, vol. 07, no. 01, pp. 16-21, Feb. 2025, doi: 10.32734/jotp.v7i1.19717.

ABSTRACT

This study investigates the structural and vibrational properties of Cu-Ag-In-S/CdSe core/shell quantum dots (QDs) deposited on mesoporous TiO_2 (mp-TiO_2) substrates using Raman spectroscopy and 3D Raman mapping. The Raman spectra of Cu-Ag-In-S/CdSe core/shell QDs revealed distinct vibrational modes of $AgInS_2$, and CdSe, compared to Cu-Ag-In-S, with notable shifts observed in the A_1 mode (282.2 cm⁻¹ to 260.8 cm⁻¹), E and B_2 modes (316.7 cm⁻¹ to 326.4 cm⁻¹), and an additional Cu-S mode (298.3 cm⁻¹ to 283.4 cm⁻¹). These shifts indicate significant interactions between the QDs and the substrate, as well as the presence of Cu and CdSe phases. 3D mapping provided spatial distribution data, showing enhanced QD incorporation and morphological variations across the substrate, with darker regions signifying Cu-enriched areas. The alterations in the Raman spectrum suggest strong interactions between Cu-Ag-In-S and CdSe. The findings contribute to a deeper understanding of the Cu-Ag-In-S /CdSe QDs, highlighting their potential for optoelectronic applications.

Keywords: Cu-Ag-In-S Quantum Dots, Core/Shell Structure, 3D Raman Mapping, Nanomaterial Characterization, Optoelectronic Materials

ABSTRAK

Penelitian ini menyelidiki sifat struktural dan vibrasi dari quantum dots (QDs) Cu-Ag-In-S/CdSe dengan struktur inti/cangkang yang dideposisikan pada substrat TiO_2 mesopori (mp-TiO_2) menggunakan spektroskopi Raman dan pemetaan 3D Raman. Spektrum Raman dari QDs Cu-Ag-In-S/CdSe inti/cangkang menunjukkan mode vibrasi khas dari $AgInS_2$ dan CdSe, dibandingkan dengan Cu-Ag-In-S, dengan pergeseran signifikan yang diamati pada mode A_1 (282,2 cm⁻¹ ke 260,8 cm⁻¹), mode E dan B_2 (316,7 cm⁻¹ ke 326,4 cm⁻¹), serta mode Cu-S tambahan (298,3 cm⁻¹ ke 283,4 cm⁻¹). Pergeseran ini menunjukkan adanya interaksi signifikan antara QDs dan substrat, serta keberadaan fase Cu dan CdSe. Pemetaan 3D memberikan data distribusi spasial, yang menunjukkan peningkatan integrasi QD dan variasi morfologi di seluruh substrat, dengan area yang lebih gelap menunjukkan daerah kaya Cu. Perubahan spektrum Raman menunjukkan interaksi yang kuat antara Cu-Ag-In-S dan CdSe. Temuan ini memberikan pemahaman yang lebih dalam tentang QDs Cu-Ag-In-S/CdSe, serta menyoroti potensinya untuk aplikasi optoelektronik.

Kata kunci: Cu-Ag-In-S Quantum Dots, Core/Shell Structure, 3D Raman Mapping, Nanomaterial Characterization, Optoelectronic Materials

1. Introduction

Raman spectroscopy serves as an important tool for characterizing ternary metal chalcogenides, providing a thorough examination of vibrational modes and crystal structures. This is particularly relevant for quantum dots (QDs), where size, composition, and surface modifications significantly influence their properties. The ability of Raman spectroscopy to detect subtle changes in lattice dynamics and bonding environments makes it a powerful technique for studying QDs. For example, Raman spectroscopy has been employed to analyze the Ag-In-S QDs[1–6], Cu-In-S[3], and (Cu, Ag)−In−S QDs.[7,8] These studies have shown that variations in Raman peak positions can indicate changes in the electronic band structure due to factors such as strain, defects, and compositional modifications.

Cu-Ag-In-S/CdSe core-shell QDs have demonstrated their potential as efficient solar energy materials for quantum dot-sensitized solar cells (QDSSCs) on mesoporous TiO_2 (mp-TiO_2) substrate, achieving an efficiency of 12.51% under 0.25 sun, attributed to their broad absorption range [8]. Given their promising performance, it is essential to investigate the structural and vibrational dynamics of Cu-Ag-In-S/CdSe core-shell QDs using Raman spectroscopy to gain deeper insights into their interactions with the mp-TiO_2 substrate. In our previous study on Cu-Ag-In-S/CdSe type-II core/shell QD-sensitized solar cells (QDSSCs), Raman analysis was performed for $AgInS_2$ and Cu-Ag-In-S QDs [8]. However, a comprehensive Raman analysis of Cu-Ag-In-S/CdSe type-II core/shell QDs has not yet been reported.

The synthesis of Cu-Ag-In-S QDs on mp-TiO_2 substrates, followed by the formation of CdSe shells, adds complexity to the material's vibrational dynamics. The incorporation of copper into $AgInS_2$ QDs alters the local bonding environment, resulting in Raman peak shifts and modifications in vibrational modes [8]. Furthermore, the addition of CdSe as a shell material influences the Raman spectra, often introducing new vibrational modes or altering existing ones due to interactions between the core and shell components. While several studies have reported Raman spectroscopy analyses of CdSe [13], its role as a shell material for Cu-Ag-In-S QDs remains insufficiently explored, highlighting the need for further investigation.

In this study, we employ Raman spectroscopy to investigate the structural and vibrational properties of Cu-Ag-In-S/CdSe core/shell QDs synthesized via the successive ionic layer adsorption and reaction (SILAR) method. The analysis focuses on the effects of core-shell interactions and the integration of QDs with mp-TiO_2 on the Raman signatures of the material. By examining peak shifts, full-width at half-maximum (FWHM) variations, and the emergence of new vibrational modes, this work provides a comprehensive understanding of the material's structural evolution and its implications for optoelectronic applications.

2. Methods

2.1. *Preparation of Mesoporous TiO_2 Substrates*

The mp-TiO_2 substrates were prepared on cleaned microscope glass slides (2.5 × 1.4 cm) using the doctor blade method. The width and thickness of the sample were defined using tape with a thickness of 18–20 µm. The TiO_2-coated substrates were then annealed at 500 °C for 90 minutes.[9]

2.2. *Synthesis of Quaternary Cu-Ag-In-S Quantum Dots*

The synthesis of Cu-Ag-In-S QDs was conducted using a two-stage SILAR method based on our previous report. Briefly, Cu/Ag-S seeds were deposited on mp-TiO_2 substrates, followed by the deposition of In-S seed layers on top of the Cu/Ag-S layers. The combined structure was then annealed, resulting in the formation of quaternary Cu-Ag-In-S QDs.

To grow the Cu/Ag-S seeds, the mp-TiO_2 nanoparticles was immersed in a 0.05 M ethanol solution of $Cu(NO_3)_2\cdot 3H_2O$ and $AgNO_3$ for 50 seconds, rinsed with ethanol, and dried at 40 °C. The samples were then dipped into a 0.1 M $Na_2S\cdot 9H_2O$ solution (methanol/DI water, 1:1, v/v) for 180 seconds, rinsed with methanol, and dried at 40 °C. This process constituted one SILAR cycle for Cu/Ag-S seeds and was repeated twice.

Subsequently, In-S seeds were grown on the Cu/Ag-S-coated mp-TiO_2 substrates. The samples were immersed in a 0.1 M $InCl_3$ ethanol solution for 180 seconds, rinsed with ethanol, and dried at 40 °C. They were then dipped into a 0.1 M $Na_2S\cdot 9H_2O$ solution (methanol/DI water, 1:1, v/v) for 180 seconds, rinsed with methanol, and dried at 40 °C. This process constituted one SILAR cycle for In-S seeds and was repeated seven times.

Finally, the Cu/Ag-S/In-S double-layer structure was annealed at 300 °C for 30 minutes, resulting in the formation of quaternary Cu-Ag-In-S QDs.

2.3. *Synthesis of Quaternary Cu-Ag-In-S/CdSe Core/Shell QDs*

To grow a CdSe shell on TiO_2/Cu-Ag-In-S electrodes, the SILAR method was employed. The selenium precursor solution was prepared by dissolving 0.36 g of selenium powder in 125 mL of ethanol containing 0.3 g of $NaBH_4$. The process involved immersing the mp-TiO_2/Cu-Ag-In-S substrates in a 0.1 M $Cd(CH_3COO)_2 \cdot 2H_2O$ methanol solution for 60 seconds, followed by rinsing with methanol and drying at 40 °C. The samples were then immersed in the selenium precursor solution for 90 seconds, rinsed with ethanol, and dried at 40 °C. This two-step process constituted one cycle of CdSe shell growth, and the cycle was repeated six times to achieve the desired shell thickness and composition.

2.4. Raman Spectroscopy Measurement

Raman spectroscopy was conducted using a Jasco NRS 5100 Raman spectrometer equipped with an argon-ion laser as the excitation source, operating at a wavelength of 523 nm. Spectral data were collected from powdered samples across a wavenumber range of 100 to 700 cm^{-1}, providing detailed insights into their vibrational properties.

3. Result and Discussion

3.1. Raman Spectra Analysis

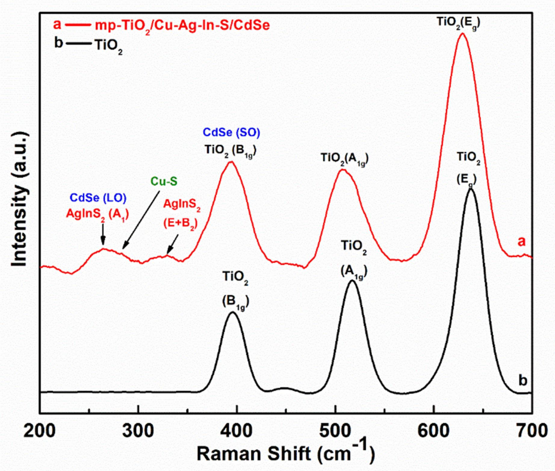

Figure 1. Raman spectra of mp-TiO_2 substrates and mp-TiO_2/Cu-Ag-In-S/CdSe

Figure 1 depicts the Raman spectra of mp-TiO_2 substrates and mp-TiO_2/Cu-Ag-In-S/CdSe. As shown in Figure 1, the Raman spectra of the samples prominently feature peaks from TiO_2 due to the direct growth of the QDs onto the mp-TiO_2 substrate. Figures 1 display the Raman peaks of anatase TiO_2, indicating three distinct vibrational modes: The 396.0 cm^{-1} peak corresponds to the B_{1g} mode, demonstrating symmetric stretching vibrations of titanium and oxygen atoms within the crystal lattice. The 517.4 cm^{-1} peak is attributed to the A_{1g} mode, representing the symmetric stretching of oxygen atoms within the lattice. The 637.2 cm^{-1} peak corresponds to the E_g mode, where the E_g mode signifies stretching vibrations of oxygen atoms against titanium atoms in the lattice.[10] The full-width at half-maximum (FWHM) measurements for these peaks are 27.33, 29.43, and 33.23, respectively. The Raman spectra of the mp-TiO_2/Cu-Ag-In-S/CdSe prominently feature peaks from TiO_2 due to the direct growth of the QDs onto the mp-TiO_2 substrate. These spectra exhibit additional small peaks in the range of 250 to 350 cm-1, corresponding to the Raman shifts for orthorhombic $AgInS_2$.

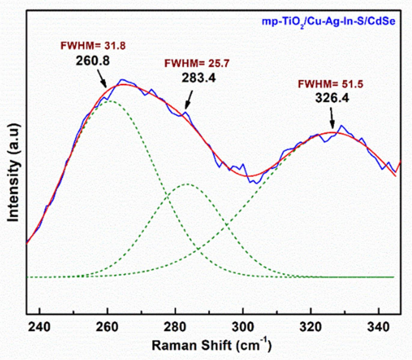

Figure 2. Enlarged Raman spectra of mp-TiO_2/Cu-Ag-In-S/CdSe in the range of ~ 230 cm^{-1} - ~340 cm^{-1}

Figure 2 presents the enlarged Raman spectra of mp-TiO_2/Cu-Ag-In-S/CdSe. In our previous report on the Raman spectra of TiO_2/Cu-Ag-In-S, Raman shift peaks were identified, including the A_1 mode peak of $AgInS_2$ at 282.2 cm^{-1} with a full width at half maximum (FWHM) of 16.9 cm^{-1}, and the E and B_2 mode peaks of $AgInS_2$ at 316.9 cm^{-1} with an FWHM of 26.2 cm^{-1}. An additional peak at 298.3 cm^{-1} was also observed, attributed to a vibrational mode associated with the chalcopyrite structure (Cu-S).[8] The current analysis reveals significant shifts in these Raman peaks. The A_1 mode peak of $AgInS_2$ at 282.2 cm^{-1} shifts to 260.8 cm^{-1} with an increased FWHM of 31.8 cm^{-1}, suggesting the presence of both the A_1 mode from $AgInS_2$ and the longitudinal optical (LO) mode from cubic CdSe, which typically occurs around 200 cm^{-1}.[11,12] Similarly, the E and B_2 mode peak of $AgInS_2$ shifts from 316.7 cm^{-1} to 326.4 cm^{-1} with an increased FWHM of 51.5 cm^{-1}, while the additional Cu-S peak shifts from 298.3 cm^{-1} to 283.4 cm^{-1}. A reduction in the intensity of the ~390 cm^{-1} mp-TiO_2 peak is also observed. This peak, now detected at 393.1 cm^{-1}, exhibits an intensity comparable to that of the peak at 510.3 cm^{-1}. The shift to 393.1 cm^{-1} is attributed to the surface optical (SO) mode of CdSe, typically found within the range of 360–380 cm^{-1}, corresponding to vibrations near the crystal surface.[13] Apart from these distinct features, minor changes are noted in the Raman shift peak and its FWHM at approximately ~500 cm^{-1}, while the peak at ~620 cm^{-1} remains unaffected. These findings provide valuable insights into the vibrational and structural dynamics of the Cu-Ag-In-S/CdSe core/shell system, including: (i) strong interfacial interactions between CdSe and Cu-Ag-In-S; (ii) Raman peak shifts and material interactions that contribute to changes in the optical and electronic properties of Cu-Ag-In-S/CdSe, as detailed in our previous publication [8]; and (iii) a decrease in the intensity of the mp-TiO_2 peak (~390 cm^{-1}), which shifts to 393.1 cm^{-1} due to the surface optical mode of CdSe, indicating a strong interaction between the QD layer and the TiO_2 substrate. This interaction can influence the electron injection mechanism from Cu-Ag-In-S/CdSe to TiO_2, a critical factor in the performance of QDSSCs.

3.2. 3D Mapping Analysis

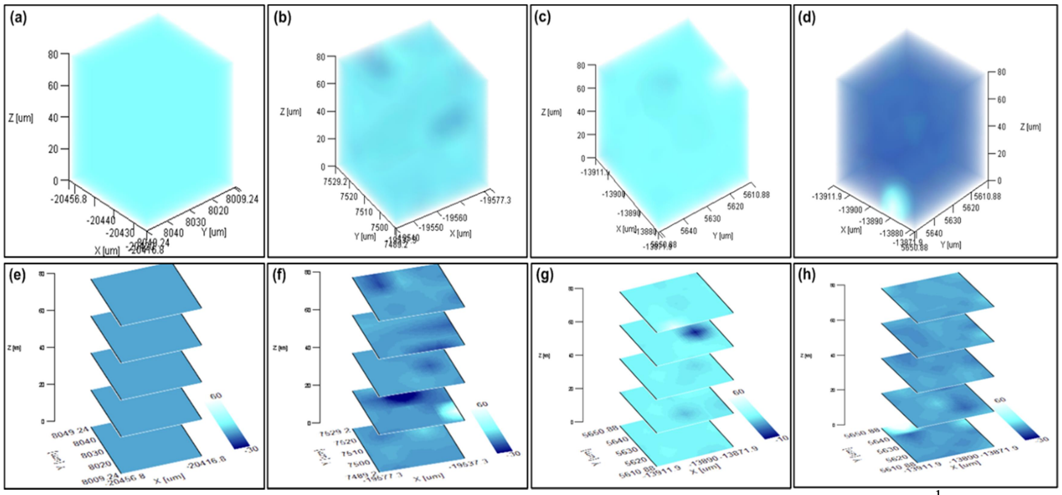

Figure 3. 3D mapping of the samples for two particular mapping areas for TiO_2 at ~620 cm^{-1} and TiO_2/QDs at ~390 cm^{-1}: (a) TiO_2/$AgInS_2$ QDs sample, (b) TiO_2/Cu-Ag-In-S QDs sample, (c) TiO_2/Cu-Ag-In-S/CdSe, (d) the 3D-mapping from the mapping areas of TiO_2 at ~620 cm^{-1} and TiO_2/Cu-Ag-In-S/CdSe at ~260 cm^{-1}; The layer-by-layer stacking of TiO_2/QDs samples determined based on the peak ratio of (e) TiO_2 to TiO_2/$AgInS_2$ QDs, (f) TiO_2 to TiO_2/Cu-Ag-In-S QDs, and (g) and (h) TiO_2 to TiO_2/Cu-Ag-In-S/CdSe QDs.

To assess the distribution of synthesized QDs within the mp-TiO_2 substrates, 3D mapping based on Raman spectra was conducted. Two specific mapping areas were compared: one for TiO_2 at ~620 cm^{-1} (representing E_g mode of TiO_2) and another for TiO_2/QDs at ~390 cm^{-1} (comprising the SO mode of CdSe, B_2 of $AgInS_2$, and B_{1g} of TiO_2). This mapping allowed the analysis of QD distribution within the TiO_2 matrix. Additionally, for the Cu-Ag-In-S/CdSe core/shell QDs sample, mapping was also performed at ~620 cm^{-1} (E_g of TiO_2) and ~260 cm^{-1} (A_1 mode of $AgInS_2$ and LO mode of CdSe) to further characterize the distribution. The layer-by-layer stacking of the TiO_2/QDs sample was also provided. Figure 3 presents the obtained results.

For comparison, 3D mapping of mp-TiO_2/$AgInS_2$ QDs sample and TiO_2/Cu-Ag-In-S QDs sample are also featured. Figures 3(a) and 3(e) illustrate the 3D mapping of the mp-TiO_2/$AgInS_2$ sample, where the color variation fails to distinctly represent the distribution of $AgInS_2$ within the TiO_2 matrix. This can be attributed to overlapping peak positions, previously mentioned. Precisely, the coinciding positions of the B_2 mode of $AgInS_2$ and the B_{1g} mode of TiO_2 result in blended peaks, hindering the differentiation of individual components. Additionally, due to their low intensity, the mapping did not include peaks in the range of 250 to 350 cm^{-1}. Nevertheless, this outcome remains valuable for comparative analysis with the sample containing Cu. Figures 3(b) and 3(f) illustrate varying color intensities in different Raman signal strengths (Z-axis) across distinct positions of the sample (X and Y-axis) in the 3D mapping. This alteration in color intensities might be attributed to the revised growth kinetics following the integration of Cu into $AgInS_2$, as highlighted in the reported SEM-EDS and XRD pattern analysis.[8] Consequently, this integration increases the quantity of synthesized QDs within the TiO_2 matrix, potentially contributing to the observed variations in the mapping colors. The varied color intensities observed in this study imply several possibilities: (i) Darker regions signify higher Cu concentrations within the $AgInS_2$ crystal structure, indicating potential Cu-enriched regions, suggesting Cu integration beyond mere substitution. (ii) Distinct color intensities may denote areas with altered material composition or structure due to dopant (Cu) variations, leading to unique Raman signals. (iii) Surface coverage or morphological differences in Cu-doped $AgInS_2$ QDs on TiO_2 nanoparticles could also result in varying Raman signal intensities across different areas. Figures 3(c), 3(d), 3(g), and 3(h) depict the 3D mapping of the mp-TiO_2/Cu-Ag-In-S/CdSe sample, revealing varying color intensities across different areas. These differences suggest possible surface coverage or morphological disparities attributed to the presence of CdSe shell QDs alongside the Cu-enriched region. However, the precise distinction between these components is challenging due to the overlapping peaks of $AgInS_2$ and CdSe in the figures.

4. Conclusion

The Raman analysis and 3D mapping of Cu-Ag-In-S/CdSe core/shell QDs on mp-TiO_2 substrates reveal significant structural and vibrational changes induced by Cu doping and CdSe shell formation. The observed Raman peak shifts and broadening indicate strong interactions between QDs and the TiO_2 substrate, while the presence of additional vibrational modes suggests structural modifications within the QDs. 3D mapping further highlights the heterogeneous distribution of QDs, with variations in signal intensity attributed to differences in QD composition, morphology, and surface coverage. The changes in the Raman spectrum indicate that there is a significant interaction between Cu-Ag-In-S and CdSe, which can improve the charge transfer efficiency in QDSSCs. These findings underscore the role of compositional tuning in enhancing the structural properties and performance of QDs for advanced optoelectronic applications.

References

[1] S.P. Hong, H.K. Park, J.H. Oh, H. Yang, Y.R. Do, "Comparisons of the structural and optical properties of o-AgInS 2, t-AgInS2, and c-AgIn5S8 nanocrystals and their solid-solution nanocrystals with ZnS", *Journal of Materials Chemistry*, vol. 22, pp.18939-18949, 2012.

[2] B. Cichy, R. Rich, A. Olejniczak, Z. Gryczynski, W. Strek, "Two blinking mechanisms in highly confined AgInS2 and AgInS2/ZnS quantum dots evaluated by single particle spectroscopy", *Nanoscale*, vol. 8, pp. 13493–13500, 2016.

[3] V. Dzhagan, O. Selyshchev, O. Raievska, O. Stroyuk, L. Hertling, N. Mazur, M.Y. Valakh, D.R.T. Zahn, "Phonon Spectra of Strongly Luminescent Nonstoichiometric Ag-In-S, Cu-In-S, and Hg-In-S Nanocrystals of Small Size", *Journal of Physical Chemistry C*, vol. 124, pp. 17273–17283, 2020.

[4] B. V. Lopushanska, Y.M. Azhniuk, V. V. Lopushansky, S.B. Molnar, I.P. Studenyak, O. V. Selyshchev, D.R.T. Zahn, "Synthesis from aqueous solutions and optical properties of Ag–In–S quantum dots", *Applied Nanoscience (Switzerland)*, vol. 10, pp. 2205–2212, 2020.

[5] A. Raevskaya, V. Lesnyak, D. Haubold, V. Dzhagan, O. Stroyuk, N. Gaponik, D.R.T. Zahn, A. Eychmüller, "A Fine Size Selection of Brightly Luminescent Water-Soluble Ag-In-S and Ag-In-S/ZnS Quantum Dots", *Journal of Physical Chemistry C*, vol. 121, pp. 9032–9042, 2017.

[6] B. V. Lopushanska, Y.M. Azhniuk, I.P. Studenyak, V. V. Lopushansky, A. V. Gomonnai, D.R.T. Zahn, "Optical Characterization of Colloidal AgInS2 Quantum Dots Synthesized from Aqueous Solutions", *Journal of Nano- and Electronic Physics*, vol. 14, pp. 02006-1–02006-5, 2022.

[7] O. Raievska, O. Stroyuk, Y. Azhniuk, D. Solonenko, A. Barabash, C.J. Brabec, D.R.T. Zahn, "Composition-Dependent Optical Band Bowing, Vibrational, and Photochemical Behavior of Aqueous Glutathione-Capped (Cu, Ag)-In-S Quantum Dots", *Journal of Physical Chemistry C*, vol. 124, pp. 17265–17272, 2020.

[8] S.U. Rahayu, A. Candra, J. Bin Shi, M.W. Lee, "Cu-mediated broadening of the absorption band of quaternary Cu-Ag-In-S/CdSe type-II core/shell quantum dot-sensitized solar cells with an efficiency

of 12.51% under 0.25 sun", *Sustainable Energy and Fuels*, vol. 8, pp. 3077–3091, 2024.

[9] P. Wang, S.M. Zakeeruddin, P. Comte, R. Charvet, R. Humphry-Baker, M. Grätzel, "Enhance the Performance of Dye-Sensitized Solar Cells by Co-grafting Amphiphilic Sensitizer and Hexadecylmalonic Acid on TiO2 Nanocrystals", *Journal of Physical Chemistry B*, vol. 107, pp. 14336–14341, 2003.

[10] W.F. Zhang, Y.L. He, M.S. Zhang, Z. Yin, Q. Chen, "Raman scattering study on anatase TiO2 nanocrystals", *Journal of Physics D: Applied Physics*, vol. 33, pp. 912–916, 2000.

[11] V.M. Dzhagan, M.Y. Valakh, A.E. Raevskaya, A.L. Stroyuk, S.Y. Kuchmiy, D.R.T. Zahn, "Resonant Raman scattering study of CdSe nanocrystals passivated with CdS and ZnS", *Nanotechnology*, vol. 18, pp. 285701-1–285701-6, 2007.

[12] Y.T. Nien, B. Zaman, J. Ouyang, I.G. Chen, C.S. Hwang, K. Yu, "Raman scattering for the size of CdSe and CdS nanocrystals and comparison with other techniques", *Materials Letters*, vol. 62, pp. 1555–1558, 2008.

[13] T.K. Das, P. Ilaiyaraja, C. Sudakar, "Whispering Gallery Mode Enabled Efficiency Enhancement: Defect and Size Controlled CdSe Quantum Dot Sensitized Whisperonic Solar Cells", *Scientific Reports*, vol. 8, pp. 1193-1–1193-10, 2018.